Fluid-structure interaction analysis for bow-shaped structure subjected to slamming pressure

Toh, Kimihiro
Kyushu University

Yanagihara, D.
Kyushu University

Nagayama, K.
Namura Shipbuilding Co., Ltd.

出版情報：pp.141-149, 2023-04-14. Taylor & Francis
バージョン：
権利関係：

Fluid-structure interaction analysis for bow-shaped structure subjected to slamming pressure

K. Toh & D. Yanagihara
Kyushu University, Fukuoka, Japan

K. Nagayama
Namura Shipbuilding Co., Ltd., Saga, Japan

ABSTRACT: In this study, the fluid-structure interaction (FSI) analyses utilizing the Incompressible Computational Fluid Dynamics (ICFD) solver implemented in LS-DYNA are performed. In addition, the accuracy verification not only of the fluid force calculation by water surface drop analyses using several wedge-shaped structures but also of the FSI analysis by a box-shaped structure is carried out. Assuming the bow flare slamming (BFS) behavior, the FSI analyses by the ICFD method of LS-DYNA on bow-shaped structures are also conducted. The differences of numerical results between the Arbitrary Lagrangian-Eulerian (ALE) method and the ICFD solver are investigated. The results show that the ICFD analysis gives the relatively reasonable values for time histories of fluid forces as well as pressure responses regardless of two-dimensional and three-dimensional structures. Through the comparison with theoretical values and empirical formulas, moreover, the discussions on the ICFD results are presented in detail.

1 INTRODUCTION

In recent years, ships are becoming larger to optimize operating costs, and the bow flare angle of ship hulls; especially container ships, tends to increase. As a result, large impact loads are applied to the bow structural members, and the bow flare slamming (BFS) is one of the concerns. In the phenomena of structural response under such impact loads, there is the interinfluence between fluid and structure, such as changes in impact pressure due to the structural deformation, and the fluid-structure interaction (FSI) analysis is necessary for the highly accurate strength investigation.

Regarding the BFS phenomena, the problem of water surface impact of elastic wedges has been studied for some time (ex.: Faltinsen, O.M. 2002, Luo, H. et al. 2010). Recently the three-dimensional studies with considering the hydro-elastic phenomena have been carried out as the computational technology progress (ex.: Truong, D.D. et al. 2019, 2021, 2022, Wang, S. & Soares, C.G. 2016, Yamada, Y. et al. 2017, 2018, 2019a, 2019b, 2020). Shan (Shan, W. & Soares, C.G. 2017) presented a comprehensive and detailed review of state of the art of knowledge on hull slamming.

Our research group has been used the Arbitrary Lagrangian-Eulerian (ALE) method in LS-DYNA; a commercial structural analysis software, to perform two-dimensional FSI analyses assuming the BFS behavior, and proposed an FSI analysis method using the ALE method through the evaluation procedure of the structural response by applying the obtained time histories of pressure response to a three-dimensional structure (Furuno, K. et al. 2014, 2015, Nakashima, M. et al. 2011, Yoshikawa, T. et al. 2013, 2017). In addition, the Incompressible Computational Fluid Dynamics (ICFD) solver (LSTC. 2014) has been implemented into LS-DYNA from 2012-2014, and the authors conducted a fundamental study using the ICFD method (Nagayama, K. et al. 2019).

As mentioned above, since the situation is being prepared for the FSI analysis to be performed more easily, in this study, the FSI analyses using the ICFD solver of LS-DYNA are performed. Also, the accuracy verification not only of the fluid force calculation by water surface drop analyses with some wedge-shaped structures (tow-dimensional analysis); see Section 3, but also of the FSI analysis by a water surface drop analysis with a box-shaped structure (three-dimensional analysis); see Section 4, is carried out. Assuming the BFS behavior, furthermore, the FSI analyses by the ICFD solver of LS-DYNA on bow-shaped structures (three-dimensional analysis); see Section 5, are conducted. Through these results by numerical simulations using the ICFD method in LS-DYNA and the comparison with the ALE results presented in the previous researches and/or theoretical and empirical values, the validity of analysis results by the ICFD method is discussed.

Table 1. Features of fluid analysis methods in LS-DYNA.

Solver	ALE	SPH	DEM	ICFD
Implementation year	1993-1994	2001-2002	2008-2011	2012-2014
Governing equation	Mass conservation law Momentum conservation law Energy conservation law	Mass conservation law Momentum conservation law Energy conservation law	— Momentum conservation law —	Mass conservation law Momentum conservation law —
Fluid characteristic	Compressible / Incompressible	Compressible	Incompressible	Incompressible
Computational technique	Finite volume method	Particle method	Particle method	Finite element method
Time evolution method	Explicit method	Explicit method	Explicit method	Implicit method
Space discretization procedure	Eulerian and Lagrangian	Meshfree method	Lagrangian	Eulerian and Lagrangian
Recommended element type	Hexa	Particle	Particle	Tetra
Coupling method with structure	Penalty method	Penalty method Constraint method	Penalty method Constraint method	(Automatic coupling)
Coupling	Weak	Weak	Weak	Strong / Weak
Turbulence model	—	—	—	k-ε, LES
Analysis method of free-surface flow	ALE (VOF) method	Particle method	Particle method	Level set method
Multiphase flow	Possible	Possible	Possible	Possible (2D)
Two-dimensional analysis	Possible	Possible	Impossible	Possible

2 FSI METHODOLOGIES IN LS-DYNA

LS-DYNA is a multi-physics solver, and various analysis methods other than the FEM (Finite Element Method), the ALE method, and the ICFD method are implemented. Among many analysis solvers in LS-DYNA, the features of four methods, i.e., ALE, SPH (Smoothed Particle Hydrodynamics), DEM (Discrete Element Method), and ICFD, that are often used for the fluid analysis, are summarized in Table 1. As can be seen from Table 1, the ALE method has been implemented in LS-DYNA from the very beginning, and there are many researches applying its solver function to the BFS problem. On the other hand, as the ICFD method has been newly implemented to LS-DYNA, studies using its solver function to the BFS problem are relatively limited.

The ICFD method has an advantage over other methods in terms of the computational time, because it is the only analysis solver that adopts the implicit method as the time evolution method. The ICFD method solves the incompressible Navier-Stokes equations, and can be applied when the target fluid is regarded as an incompressible fluid. A fluid can be generally considered incompressible when the Mach number is lower than 0.3, and the phenomena such as slamming or sloshing are in this range. By introducing the incompressibility hypothesis, the equation of state (EOS) is not needed to define, as the incompressible fluid has a constant density. The ICFD method, which is based on the FEM as shown in Table 1, is suitable for the phenomena with relatively small deformation on the structural members, and the coupling between fluid and structure is automatically performed. In addition, the remeshing of fluid part is automatically performed too when a fluid element is greatly deformed. The ICFD solver uses a level set method, which is based on a fast and reliable technique, as the analysis method of free-surface flow so as to track and correctly represent moving interfaces, and considers the interplay such as surface-tension effects.

In this study, based on the above points of view, the ICFD method is adopted to simulate the water impact behavior with considering the FSI effects. By the current ICFD solver of LS-DYNA, since it is difficult to stably perform the multiphase flow analysis with a large density difference such as water and air; particularly in three-dimensional analyses, the air part is treated as the void in this paper.

3 COMPARISON BETWEEN THEORETICAL / EMPIRICAL VALUES AND ALE / ICFD RESULTS REGARDING WEDGE-SHAPED (TWO-DIMENSIONAL) STRUCTURE

In this section, a series of drop analyses by the ICFD method is conducted using two-dimensional wedge-shaped structures, and the verification of the ICFD analysis is discussed through the comparison with a theoretical solution, an empirical formula, and simulation results by the ALE method.

3.1 *Theoretical solution*

Many methods have been proposed to calculate the slamming pressure on rigid bodies that penetrate the water surface with a certain velocity. As the earliest methods, Karman (von Karman, T. 1929) and Wagner (Wagner, H. 1932) are well known. Regarding the impact load when the seaplane lands on the water, Karman focused on the change in momentum due to the change in the added mass when the two-dimensional wedge plunged into the water surface, and calculated the impact load. Based on Karman's theory, on the other hand, Wagner introduced the calculation method of impact water pressure taking into account the piling up water when a two-dimensional wedge collides with the water surface. Comparing Wagner's theory with Karman's one, whether there is the piling water surface is signifi-

cant, and the impact load according to Wagner's theory is approximately larger 2.5 times, i.e., $(\pi / 2)$ squared, than that of Karman's one. In this paper, Wagner's theory, which is closer to the actual phenomena of the BFS behavior, is considered as the theoretical solution.

Wagner's theory does not consider the effect of air, and is based on the following assumptions:

- The fluid is non-viscous and incompressible.
- The gravity can be neglected because the acceleration of fluid is much greater than that of gravity.
- The draft of wedge is much smaller than the wetted width.
- The impact velocity is constant.

The pressure coefficient, C_p, based on Wagner's theory is given by Equation 1:

$$C_p = 1 + \frac{\pi^2}{4\tan^2\beta} \tag{1}$$

where β is the deadrise angle, i.e., the wedge tip angle to the water surface.

3.2 *Empirical formula*

Chuang (Chuang, S.L. 1966, 1970) carried out a large number of impact experiments using rigid and elastic bodies, and proposed an empirical formula through these experimental results (Stavovy, A.B. & Chuang, S.L. 1976).

The pressure coefficient, C_p, based on Stavovy & Chuang is given by Equation 2:

$$C_p = \frac{288k}{\cos^4\beta} \tag{2}$$

where k is a coefficient that varies with the deadrise angle, β, as follows:

$$k\begin{cases} =\dfrac{0.37\beta}{2.2}+0.5 \text{ (0 deg. } \le \beta \le \text{ 2.2 deg.)} \\ =2.1820894-0.9451815\beta+0.203754\beta^2-0.0233896\beta^3 \\ +0.0013578\beta^4-0.00003132\beta^5 \text{ (2.2 deg. } \le \beta \le \text{ 11 deg.)} \\ =4.748742-1.3450284\beta+0.1576516\beta^2-0.0092976\beta^3 \\ +0.0002735\beta^4-0.00000319864\beta^5 \text{ (11 deg. } \le \beta \le \text{ 20 deg.)} \\ =\dfrac{0.76856471}{288}\left(1+\dfrac{2.4674}{\tan^2\beta}\right) \text{ (20 deg. } \le \beta) \end{cases} \tag{3}$$

3.3 *Numerical simulation by ALE*

Authors' research group has used the ALE method in LS-DYNA to perform two-dimensional FSI analyses assuming the BFS phenomena.

Yoshikawa et al. (Furuno, K. et al. 2014, 2015, Nakashima, M. et al. 2011, Yoshikawa, T. et al. 2013, 2017); former colleagues of authors, performed the FSI analyses under the BFS load to calculate the impact pressure and the structural response accurately. In these studies, the ALE method in LS-DYNA, which can simulate the fluid-structure coupling behavior, was applied for the impact problem of elastic wedges varying their deadrise angle. In these ALE analyses, two types of modeling for the air part were considered. One was modeling the air part with the fluid assuming air, and the other was modeling that with the void.

As for the detailed information about these FSI analyses utilizing the ALE method in LS-DYNA, e.g., the calculation model and its mesh size for FEM, the calculation conditions, the material and physical properties of structure and fluid, and so on, please see the references (Furuno, K. et al. 2014, 2015, Nakashima, M. 2011, Yoshikawa, T. et al. 2013, 2017).

3.4 *Numerical simulation by ICFD*

In order to investigate the simulation accuracy of the ICFD method in LS-DYNA, the drop analyses on the water surface using two-dimensional wedge-shaped structures varying their deadrise angle are conducted.

The model for the ICFD analysis is shown in Figure 1. Each mesh size of fluid and structural parts is determined based on the results of convergence calculations as well as previous studies with the ALE analysis, and that of fluid around structure is approximately 1 mm. Although the wedge-shaped structures are modeled by an elastic body assuming a material of steel, they can be almost regarded as a rigid body because two-dimensional solid elements are utilized in this simulation. As shown in Figure 1, the fluid part is only water, and the air part is treated as the void due to keeping the analysis stability. Table 2 shows the material and physical properties of structure (elastic body) and fluid (water) in this ICFD analysis. As the boundary conditions, the left, right, top, and bottom edges of the analysis model are free-slip boundaries, and the boundary between fluid and structure is a non-slip boundary. The drop analyses varying the deadrise angles, β, as 1, 2, 3, 5, 10, 15, and 30 degrees are performed under the initial velocity of 6.15 m/s, and the gravitational effects are not considered this time not only for comparison with Wagner's theory but also for simplicity.

An example of the slamming behavior to the water surface simulated by the ICFD analysis is shown in Figure 2. From Figure 2, it is found that the FSI analysis with the water splash can be performed.

As shown in Equation 4, the dimensionless value of the maximum impact pressure, $P_{\max}$, which is obtained by the ICDF analysis, is considered as the pressure coefficient, C_p.

$$C_p = \frac{P_{\max}}{\frac{1}{2}\rho_f v^2} \tag{4}$$

where ρ_f and v are the density of fluid (water) and the velocity, respectively. As the velocity, v, the initial velocity, i.e., 6.15 m/s, is adopted instead of the relative impact velocity between fluid and structure.

Figure 3 shows the comparison between the pressure coefficients, C_p, given by Equations 1-2 and 4. Based on the results obtained by the ALE analyses performed in the previous researches (Furuno, K. et al. 2014, 2015, Yoshikawa, T. et al. 2017), the pressure coefficients, C_p, are calculated in the same way as Equation 4, and these results are also plotted in Figure 3. In Figure 3, solid and open square marks of the ALE results represent whether or not the air is considered.

As can be seen from Figure 3, the ALE results without considering the air; that is, the air part is considered as the void, almost agree with Wagner's theory. In contrast, the ALE results with considering the air effect almost agree with the empirical formula by Stavovy & Chuang. It can be also seen that the ICFD results and the empirical formula by Stavovy & Chuang are in good agreement except for the small range of the deadrise angle, β.

When the deadrise angle, β, is 2 degrees or less, the value of pressure coefficient, C_p, decreases due to occurring the air entrainment in the empirical formula by Stavovy & Chuang. This phenomenon caused by the air cushion effects can be simulated by the ALE analysis with considering the air, but not by the ICFD analysis, because the air part in the ICFD analysis should be modeled by not air but void to proceed with the stable calculations in the current LS-DYNA.

When the deadrise angle, β, is very small, the difference of the pressure values obtained with and without air is relatively large, so it is necessary to consider the air cushion effects so as to calculate the accurate impact pressure. Whereas, when the deadrise angle, β, is 2 degrees or more, the difference due to the air cushion effects is hardly observed between the ICFD results and the ALE results with considering the air in Figure 3, and the ICFD results show almost the same values as the experimental value by Stavovy & Chuang.

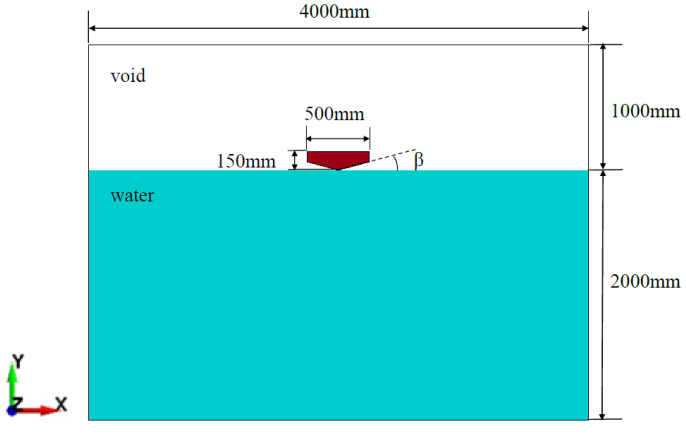

Figure 1. Model for ICFD analysis of wedge-shaped structure.

Table 2. Material and physical properties.

(a) Structure (elastic body)

Item	Symbol	Value	Unit
Young's modulus	E	206000	MPa
Poisson's ratio	ν	0.3	—
Density	ρ_s	7.85×10^{-9}	ton/mm^3

(b) Fluid (water)

Item	Symbol	Value	Unit
Viscosity coef.	η	1.5674×10^{-9}	MPa· s
Density	ρ_f	1.00×10^{-9}	ton/mm^3

Figure 2. Example of slamming behavior obtained by ICFD analysis at deadrise angle of 30 degrees.

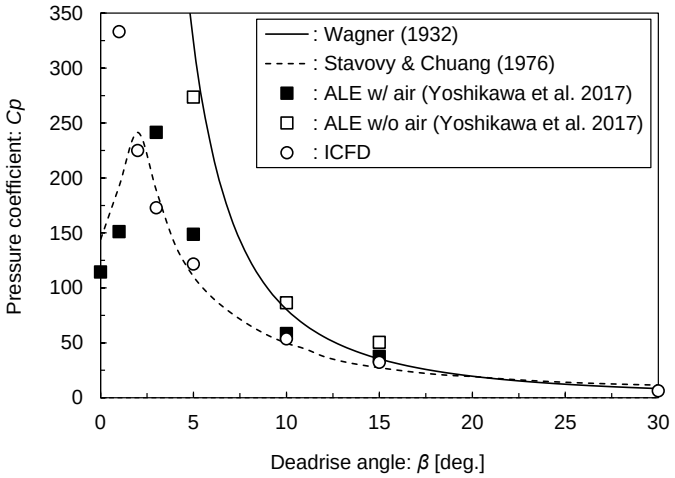

Figure 3. Relationships between pressure coefficient, C_p, and deadrise angle, β.

From these results, except for the range where the deadrise angle, β, is very small, it can be confirmed that the ICFD analysis gives the relatively reasonable value about the fluid force of the two-dimensional structure.

4 ICFD ANALYSIS FOR BOX-SHAPED (THREE-DIMENSIONAL) STRUCTURE

Truong (Truong, D.D. et al. 2019) used the ALE method of LS-DYNA to analyze the drop experiment of a box-shaped structure conducted by Mori (Mori, K. 1977). In this section, therefore, the similar analysis is carried out using the ICFD method, and the simulation accuracy of the three-dimensional analysis and the validity of the FSI analysis are investigated by comparing the ICDF results with not only the ALE results by Truong et al. but also the experimental results by Mori.

4.1 *Analysis model and conditions*

Figure 4 shows the model for the ICFD analysis created with reference to the analysis model utilizing Truong et al. based on Mori's experimental works. The FE model including the internal members, such as longitudinal stiffeners, of the box-shaped structure is indicated in Figure 5, in which the upper plate is hidden so that the internal members can be confirmed. This box-shaped structure has two tee-bar stiffeners, and their dimensions are 94 × 6 + 56 × 6 mm. The structure is modeled by the elastic body, and its mesh size is about 10 mm × 10 mm. Table 3 shows the material and physical properties of structure (elastic body) and fluid (water) in this ICFD analysis.

The boundary conditions are free-slip boundaries around the fluid part and a non-slip boundary between fluid and structure. Analysis model and conditions other than the above are almost same as those described in Section 3.4. The structural responses are obtained from the ICFD analysis when the box-shaped structure freely falls from a height of 300 mm above the water surface.

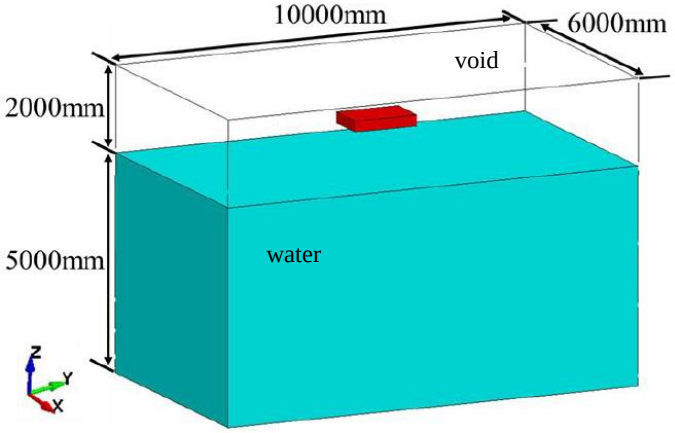

Figure 4. Model for ICFD analysis of box-shaped structure.

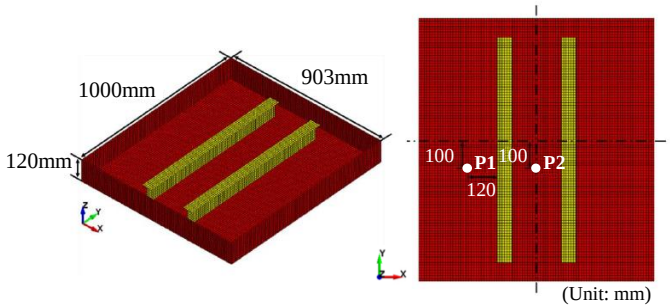

Figure 5. FE model of box-shaped structure.

Table 3. Material and physical properties.

(a) Structure (elastic body)

Item	Symbol	Value	Unit
Young's modulus	E	68700	MPa
Poisson's ratio	ν	0.3	—
Density	ρ_s	2.7×10^{-9}	ton/mm^3

(b) Fluid (water)

Item	Symbol	Value	Unit
Viscosity coef.	η	1.5674×10^{-9}	MPa· s
Density	ρ_f	1.00×10^{-9}	ton/mm^3

4.2 *Analysis results and discussion*

The comparisons of impact pressure causing at two evaluation points, i.e., P1 and P2 shown in the right figure of Figure 5, between the experiment by Mori, the ALE results presented by Truong et al., and the ICFD results are indicated in Figure 6. It should be noted that the effect of air is considered in the ALE analysis by Truong et al. shown in Figure 6.

In Figure 6, the ICFD results are larger than the ALE and the experimental results at both evaluation points. In this ICFD analysis, the air is not considered, while in the ALE analysis by Truong et al., the air was properly modeled, and the air cushion effects also existed in the experimental results by Mori. By contrast to the ALE and the experimental results, consequently, the phenomenon of pressure reduction due to the entrainment of air does not occur in the ICFD analysis, so it is considered that the ICFD results show the relatively larger pressure values. Here, this analysis corresponds to the case where the deadrise angle, β, is zero. As can be seen from the results in Section 3, therefore, this is the most remarkable case where the ICFD method indicates the larger pressure values. However, in all ICFD, ALE, and experimental results, an almost similar tendency can be observed that the pressure fluctuation gradually decreases with the oscillation after reaching the peak pressure.

Truong et al. also performed the ALE analysis without considering the air; namely with the air part as the void. Figure 7 shows the comparison of the impact pressure at P2 obtained by the ALE and the ICFD simulations, which do not consider the air effect. From Figure 7, when the air is not taken into account in the ALE analysis, as the maximum pressure value of the ICFD and the ALE results are almost the same, the analytical accuracy of the ICFD method may be the same level as the ALE method.

From the above, it can be confirmed that the time histories of impact pressure by the ICFD method show the same trend as the ALE and the experimental results. In other words, although it is necessary to pay attention to the fact that the ICFD analysis gives higher pressure values in the range where the deadrise angle, β, is very small, the ICFD analysis gives the relatively reasonable results even under the three-dimensional and the FSI influences.

5 ICFD ANALYSIS FOR BOW-SHAPED (THREE-DIMENSIONAL) STRUCTURE

Through the several investigations in the previous sections, it can be confirmed that the ICFD analysis enables the relatively valid FSI analyses about both two-dimensional and three-dimensional structures. In this section, thus, a series of drop analyses by the ICFD method is carried out using three-dimensional bow-shaped structures of an actual ship.

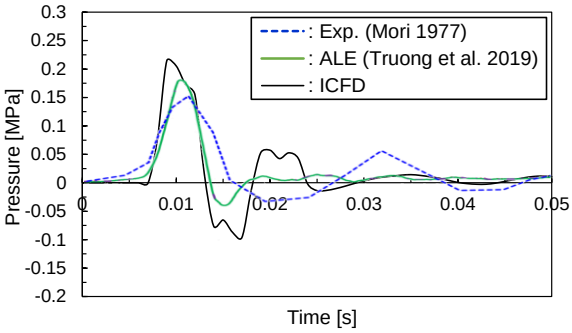

(a) Evaluation point: P1

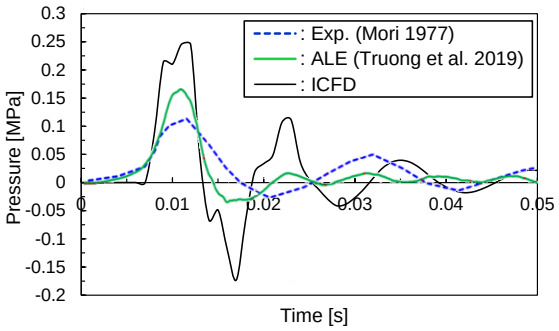

(b) Evaluation point: P2

Figure 6. Comparisons of pressure-time histories between experiment by Mori, ALE w/ air by Truong, and ICFD. (This case corresponds to $\beta = 0$.)

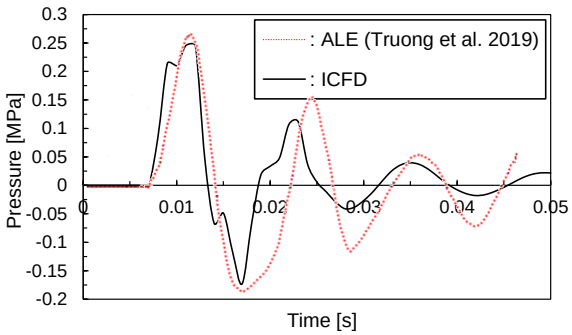

Figure 7. Comparison of pressure-time histories at evaluation point P2 between ALE w/o air (void) by Truong and ICFD.

5.1 *Analysis model and conditions*

Figure 8 shows the model for the ICFD analysis of the bow-shaped structure. The FE model including the internal members, such as transverse frames and longitudinal stiffeners, of the bow-shaped structure is indicated in Figure 9, in which the front plate is hidden so that the internal members can be confirmed. As for the modeling of the bow-shaped structure, since it is difficult to model and analyze a wide or whole area of an actual bow part, the ICFD analyses are performed for simplicity using bow-shaped structures whose shapes do not change in the longitudinal direction this time. The yellow area surrounded by white dotted lines shown in right figure of Figure 9 is the region for evaluating structural response, and the modeling range in the longitudinal direction is five times longer than this evaluating region. The bow shape of the FE model and its dimensions are determined based on an actual 14000 TEU container ship. The hull plates and other large plate members or the longitudinal stiffeners are modeled by shell or beam elements, respectively. The structure is modeled by the elastic body, and its mesh division around the region for evaluating structural response is five between each longitudinal stiffener space. Three FE models with flare angles of 25, 30, and 37 degrees are used for this ICFD simulation. The flare width of 11.2 m is constant, so the height of bow-shaped structure, which is about 30 m, slightly changes when the flare angle changes. Table 4 shows the material and physical properties of structure (elastic body) and fluid (water) in this ICFD analysis.

The boundary conditions or analysis model and conditions other than the above are completely or almost the same as those described in Section 4.1 or Section 3.4, respectively. Using the FE models with different flare angles, a series of drop analyses is performed varying the forced velocities of 5, 7.5, 10, and 15 m/s.

5.2 *Analysis results and discussion*

Using the maximum value of the impact pressure in the evaluating region of flare plate seen in Figure 9, the pressure coefficients, C_p, obtained by the ICFD analyses are calculated from Equation 4. As the velocity, v, each forced velocity is adopted instead of the relative impact velocity between fluid and structure. The comparisons between these pressure coefficients, C_p, based on the ICFD results, Wagner's theoretical solution, and Stavovy & Chuang's empirical formula are shown in Figure 10.

As can be seen from Figure 10, the pressure coefficients, C_p, by the ICFD method are slightly smaller than the empirical formula by Stavovy & Chuang as the flare angle increases. The empirical formula targets two-dimensional wedge-shaped structures, whereas this ICFD analysis targets three-dimensional structures. In the ICFD analysis, hence, the impact pressure decreases due to the escape of fluid in the longitudinal direction. Although there are slight differences in the pressure coefficients, C_p, the ICFD results generally agree with Wagner's theoretical solution and Stavovy & Chuang's empirical formula, so it is considered that the ICFD analysis provides the relatively appropriate pressure values.

The theoretical value of the bending stress causing in an element, which is here expressed by '*Elm-A*', located in the center of the evaluating region is obtained by the following procedure:

(1) Find the time when von Mises stress in *Elm-A* reaches the maximum value.

(2) At the time of (1), obtain the total pressure value causing in the panel, which includes *Elm-A*, surrounded by both longitudinal and transverse structural members from the ICFD results.

(3) For a rectangular panel with fixing its four sides under the uniformly distributed pressure, which is given as the average value of the total pressure ac-

quired in (2), derive the maximum bending stress in the X- and Y-directions.

The X- and Y-directions use the element coordinate system, and correspond to the ship length and depth directions, respectively. The bending stresses calculated by each stress in the X- and Y-directions on upper and lower surfaces of *Elm-A* are also obtained from the ICFD results. Table 5 shows the comparisons between the theoretical values according to the above procedure and the ICFD results at the forced velocity of 15 m/s.

It can be confirmed that the errors of the ICFD results with respect to the theoretical values are almost less than 10% in Table 5, so the bending stress obtained from the ICFD analysis can be seen a reasonable value. From these results, if the impact pressure acting on the hull plate of flare part in the BFS behavior can be accurately estimated, it is possible to estimate the stress based on the deformation theory of the plate with fixing its circumference.

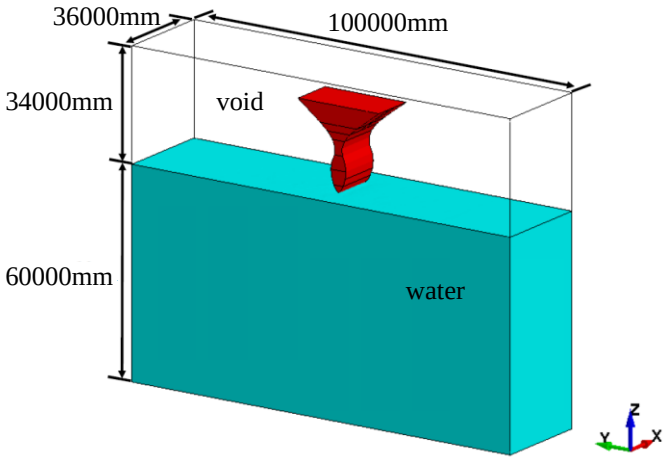

Figure 8. Model for ICFD analysis of bow-shaped structure.

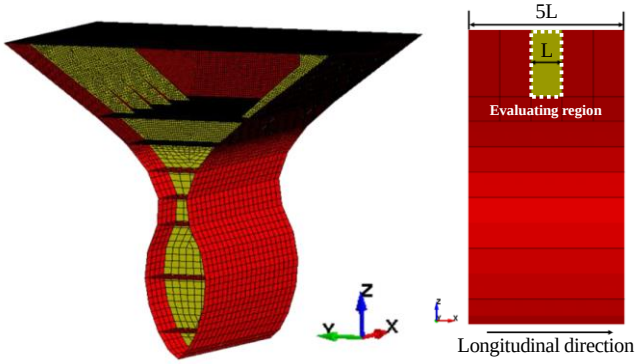

Figure 9. FE model of bow-shaped structure.

Table 4. Material and physical properties.

(a) Structure (elastic body)

Item	Symbol	Value	Unit
Young's modulus	E	206000	MPa
Poisson's ratio	ν	0.3	—
Density	ρ_s	9.116×10^{-9}	ton/mm^3

(b) Fluid (water)

Item	Symbol	Value	Unit
Viscosity coef.	η	1.5674×10^{-9}	MPa· s
Density	ρ_f	1.00×10^{-9}	ton/mm^3

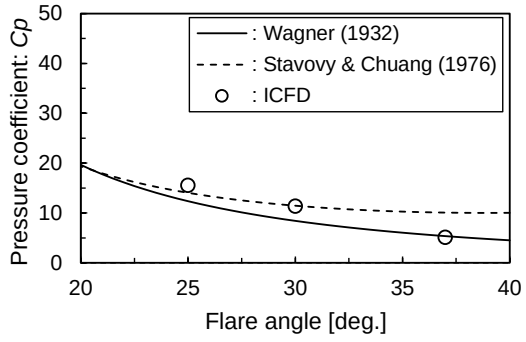

(a) 5 m/s

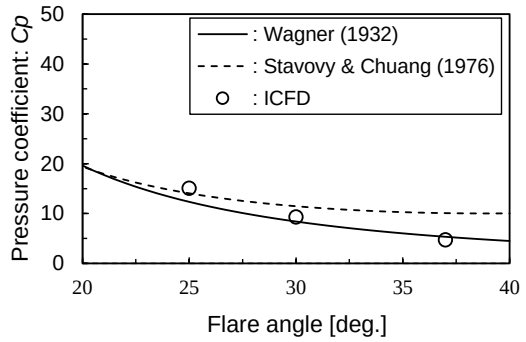

(b) 7.5 m/s

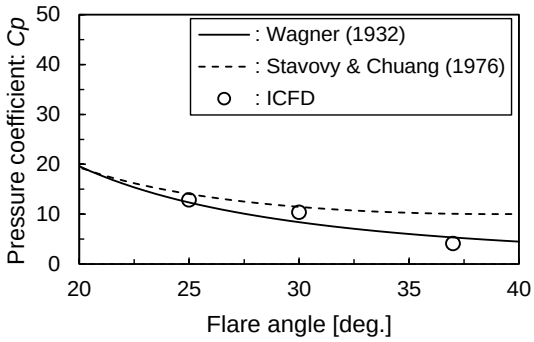

(c) 10 m/s

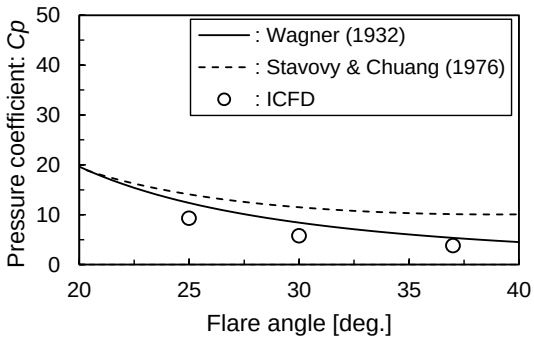

(d) 15 m/s

Figure 10. Relationships between pressure coefficient, C_p, and flare angle.

Table 5. Comparisons of bending stresses between theoretical value and ICFD result at forced velocity of 15 m/s.

(a) X-direction

Flare angle [deg.]	Theoretical [MPa]	ICFD [MPa]	Error [%]
25	152.1	164.0	+7.8
30	101.5	112.2	+10.5
37	62.1	70.4	+6.7

(b) Y-direction

Flare angle [deg.]	Theoretical [MPa]	ICFD [MPa]	Error [%]
25	506.9	488.3	-3.7
30	338.3	351.9	+4.0
37	207.1	221.0	+6.7

6 CONCLUSIONS

In the present paper, using the ICFD solver in LS-DYNA, the fluid analyses as well as the FSI analyses with wedge-, box-, and bow-shaped structures were performed. In this study, the following findings can be drawn:

- Comparing the results by the drop analyses of wedge-shaped structures with the theoretical solution and the empirical formula, the fluid force calculation by the ICFD analysis has the enough accuracy.
- Comparing the results by the drop analysis of a box-shaped structure with the ALE results, the ICFD analysis gives relatively reasonable results even under the three-dimensional and the FSI effects.
- Comparing the impact pressure and the bending stress obtained from the drop analyses of bow-shaped structures with the theoretical and the empirical values, the ICFD analysis provides relatively appropriate structural responses.

Based on the above results, the feasibility of the stress estimation in the BFS behavior by the ICFD analysis was demonstrated, but present findings are applied to specific conditions examined this time. It is pointed out that further studies are necessary to obtain more general conclusions. As future works, it is necessary to perform the ICFD analysis considering more realistic situations as follows:

- Actual wave shape
- Shape change of bow part in longitudinal direction
- Elasto-plastic structure

In the future, it is desirable to develop the stress evaluation method in the BFS behavior that does not require the numerical simulations such as the ALE or the ICDF analysis.

ACKNOWLEDGMENTS

This work was supported by JSPS KAKENHI Grant Number JP21K04523. Furthermore, this research was partly performed with the supports of JSPS KAKENHI Grant Number JP20K14960 and Grant-in-aid of the Fundamental Research Developing Association for Shipbuilding and Offshore (REDAS). The authors are grateful to JSPS and REDAS for their supports.

REFERENCES

Chuang, S.L. 1966. Slamming of rigid wedge-shaped bodies with various deadrise angles. *NSRDC Report* 2268.

Chuang, S.L. 1970. Investigation of impact of rigid and elastic bodies with water. *NSRDC Report* 3248.

Faltinsen, O.M. 2002. Water Entry of a Wedge with Finite Deadrise Angle. *Journal of Ship Research* 46(1): 39-51.

Furuno, K., Maeda, M. & Yoshikawa, T. 2014. The effects of wave surface and trapped air on the impact pressure at bow flare slamming. *Proceedings of the 28th Asian-Pacific Technical Exchange and Advisory Meeting on Marine Structures*: 120-129.

Furuno, K., Maeda, M. & Yoshikawa, T. 2015. The effect of Fluid Behavior on Structural Response under Bow Flare Slamming Load. *Conference Proceedings, The Japan Society of Naval Architects and Ocean Engineers* 20:299-302 (in Japanese).

LSTC. 2014. ICFD THEORY MANUAL Incompressible fluid solver in LS-DYNA.

Luo, H., Hu, J. & Soares, C.G. 2010. Numerical simulation of hydroelastic responses of flat stiffened panels under slamming loads. *Proceedings of the ASME 2020 39th International Conference on Ocean, Offshore and Arctic Engineering*: 373-381.

Mori, K. 1977. Response of the Bottom Plate of High Speed Crafts under Impulsive Water Pressure. *Journal of the Society of Naval Architects of Japan* 142: 297-305 (in Japanese).

Nagayama, K., Toh, K. & Yanagihara, D. 2019. Fluid-Structure Interaction Analysis for Structures with Various Shapes Subjected to Slamming Impact Pressure. *Conference Proceedings, The Japan Society of Naval Architects and Ocean Engineers* 29:415-418 (in Japanese).

Nakashima, M., Maeda, M. & Yoshikawa, T. 2011. A Study of Water Impact Problem Utilizing Numerical Simulation Considering Fluid-Structure Interaction. *Proceedings of the 25th Asian-Pacific Technical Exchange and Advisory Meeting on Marine Structures*: 309-316.

Shan, W. & Soares, C.G. 2017. Review of Ship Slamming Loads and Responses. *Journal of Marine Science and Application* 16: 427-445.

Stavovy, A.B. & Chuang, S.L. 1976. Analytical determination of slamming pressures for high speed vessels in waves. *Journal of Ship Research* 20(4): 190-198.

Truong, D.D., Jang, B-S., Ju, H-B., Han, S.W. & Han, S. 2019. A Study on Dynamic Response of Flat Stiffened Plates to Slamming Loads Considering Fluid-Structure Interaction. *Practical Design of Ships and Other Floating Structures*: 75-99.

Truong, D.D., Jang, B-S., Ju, H-B. & Han, S.W. 2021. Prediction of slamming pressure considering fluid-structure interaction. Part II: Derivation of empirical formulations. *Marine Structures* 75: 102700.

Truong, D.D., Jang, B-S., Ju, H-B. & Han, S.W. 2022. Prediction of slamming pressure considering fluid-structure interaction. Part I: Numerical simulations. *Ships and Offshore Structures* 17(1): 7-28.

von Karman, T. 1929. The impact on seaplane floats during landing. *National Advisory Committee for Aeronautics*. Technical Note No. 321.

Wagner, H. 1932. Uber Stossund Gleitvergange an der Oberflache von Flussigkeiten. *Zeitschrift fuer Angewandte Mathematik und Mechanik* 12: 193-215.

Wang, S. & Soares, C.G. 2016. Experimental and numerical study of the slamming load on the bow of a chemical tanker in irregular waves. *Ocean Engineering* 111: 369-383.

Yamada, Y. & Kameya K. 2017. A fundamental study on the dynamic response of hull girder of container ships due to slamming load. *Proceedings of the ASME 2017 36th International Conference on Ocean, Offshore and Arctic Engineering*. OMAE2017-61068.

Yamada, Y. & Kameya K. 2018. A study on the dynamic ultimate strength of global hull girder of container ships subjected to hogging moment. *Proceedings of the ASME 2018 37th International Conference on Ocean, Offshore and Arctic Engineering*. OMAE2018-77402.

Yamada, Y. 2019a. Approach to simulate dynamic elasto-plastic whipping response of global hull girder of a large container ship due to slamming load. *Proceedings of the Twenty-ninth (2019) International Ocean and Polar Engineering Conference* 3: 2808-2816.

Yamada, Y. 2019b. Dynamic Collapse Mechanism of Global Hull Girder of Container Ships Subjected to Hogging Moment. *Journal of Offshore Mechanics and Arctic Engineering* 141(5): 051605.

Yamada, Y., Takamoto, K., Nakanishi, T., Chong, M. & Komoriyama, Y. 2020. Numerical study on the slamming impact of stiffened flat panel using ICFD method: Effect of structural rigidity on the slamming impact. *Proceedings of the ASME 2020 39th International Conference on Ocean, Offshore and Arctic Engineering*. OMAE2020-18242.

Yoshikawa, T. & Maeda, M. 2013. Numerical simulation of structural response under bow flare slamming load. *Proceedings of the 4th International Conference on Marine Structures*: 25-33.

Yoshikawa, T., Miyake, R., Yoshida, T. & Maeda, M. 2017. Numerical Simulation of Structural Response under Bow Flare Slamming Load. *Journal of the Japan Society of Naval Architects and Ocean Engineers* 26: 267-276 (in Japanese).